Characterization and catalytic activities of MoMCM-41

Deug-Hee Cho [a,*], Tae-Sun Chang [a], Seung-Kon Ryu [b] and Young K. Lee [a]

[a] *Advanced Chemical Technology Division, Korea Research Institute of Chemical Technology, 100 Jang-Dong, Yusong-Gu, Taejon 305-343, Korea*
[b] *Department of Chemical Engineering, Chungnam University, Gung-Dong, Yusong-Gu, Taejon 305-764, Korea*

Received 14 August 1999; accepted 26 November 1999

Catalysts consisting of molybdenum incorporated into MCM-41 mesoporous molecular sieves (MoMCM-41) were synthesized and characterized by XRD, N_2 adsorption/desorption, ESR, FTIR, and UV-vis analysis techniques. The MoMCM-41 catalysts were synthesized by addition of $Na_2MoO_4{\cdot}2H_2O$ as molybdenum source at the initial step of synthesis; the framework Mo in MoMCM-41 catalysts could be confirmed by ESR, FTIR and UV-vis. As the molybdenum content is increased, the structure of MoMCM-41 changed from hexagonal to amorphous. Molybdenum loading up to ca. 10% was a maximum concentration that was obtained in this study. The MoMCM-41 catalysts showed a catalytic activity for propylene oxidation.

Keywords: MoMCM-41, framework Mo, oxidation of propylene

1. Introduction

A new class of mesoporous silica tube-like materials designated as MCM-41 was reported in 1992 [1–3]. MCM-41 materials possess a hexagonal arrangement of uniformly sized unidimensional mesopores. An exciting property of these materials is the possibility of controlling the internal diameter of the mesopores between 2 and 10 nm by varying the chain length of the micellar surfactant template [3,4]. Their high thermal and hydrothermal stability, uniform size and shape of the pores, and large surface areas, make them of interest as catalysts and adsorbents [1–4].

Many researchers investigated MCM-41 materials in which a catalytically active component was introduced. Several elements, including Al [5,6], Ti [7], V [8,9], B [10,11], Mn [12,13], Ta [14], Cu [15], Fe [16], Cr [17] and Ga [18], have been said to be incorporated into the framework in order to generate potential catalytic activity. A few papers have dealt with the local structural characteristics of metal ions in MCM-41 materials [19–23].

Because the molybdenum has redox properties, molybdenum-substituted MCM-41 was synthesized by addition of potassium molybdate [24] or sodium molybdate [25] as the metal ion precursors. As an example, molybdenum supported on mesoporous material such as Mo/Al-MCM-41 used for hydrodemetallization of nickel tetraphenylporphyrin showed catalytic activity [26]. In addition, NiMo/MCM-41 catalysts were prepared to study the hydrocracking vacuum gasoil reaction [27] and hydrodesulfurization [28]. However, there was not reported a systematic research to examine molybdenum incorporated into silica MCM-41 at the initial step of synthesis (so-called "direct synthesis method").

In this work, various MoMCM-41 catalysts were synthesized by using a direct synthesis method in order to incorporate molybdenum into framework positions of MCM-41 and characterized by using several analytical tools. Their catalytic performance was tested for oxidation of propylene.

2. Experimental

2.1. Synthesis of MoMCM-41

For this study, the synthesis procedure of MoMCM-41 catalysts was based on the procedure described in [29], and involved mixing sodium silicate and cetyltrimethyl ammonium chloride (CTACl) template.

A gel with a molar composition of $CTACl : 0.15\ (NH_4)_2O : 4SiO_2 : Na_2O : xMoO_3 : 200H_2O$ was prepared by using Ludox AS (DuPont) as the silicon source, CTACl (Aldrich, 25 wt% solution in water) as the surfactant and NaOH (Aldrich) as OH^- source. $Na_2MoO_4{\cdot}2H_2O$ (Junsei) served as the metal precursor and $EDTANa_4$ solution (33.3 wt%) served as a salt adding to the gel during hydrothermal reaction. The 30 wt% acetic acid was used to adjust the pH of the gel. Ludox AS (40 wt% SiO_2, 0.16 wt% NH_3, 0.08 wt% Na_2O, 59.8 wt% H_2O) was dissolved in an excess of aqueous NaOH solution to obtain a clear solution of sodium silicate (Na/Si = 1/2). The sodium silicate was added drop by drop to a propylene bottle containing CTACl and NH_4OH solution with vigorous magnetically stirring at room temperature for 10 min. After 30 min of vigorous stirring, the necessary amount of $Na_2MoO_4{\cdot}2H_2O$ solution was added dropwise to the gel and stirring was continued for another 30 min to obtain a homogeneous gel. The gel was heated to 373 K for 1 day for hydrothermal reaction. Then, the procedure after

* To whom correspondence should be addressed.

this follows the method in [29]. Si/Mo ratios of calcined samples were determined by AA.

2.2. Characterization

X-ray powder diffraction patterns for the as-synthesized and calcined samples were obtained on an Rigaku 215D6 instrument using monochromatic Cu K_α radiation. It was operated at 35 kV and 15 mA. The experimental conditions correspond to a conventional step width of 0.016° and scan speed of 5°/min.

Surface areas and N_2 adsorption–desorption isotherms on the samples were measured on a Micromeritics ASAP-2400 apparatus using super-pure nitrogen (99.999%) as adsorbate at 77 K. Samples (about 100 mg) were pre-outgassed overnight at 573 K under vacuum (10^{-5} Torr). The surface area was calculated by BET equation at the range of $P/P_0 = 0$–0.25. The total pore volume was calculated at above $P/P_0 = 0.99$. The size of framework-confined mesopores was determined by BJH analysis [30] of the nitrogen desorption isotherms.

X-band ESR spectra were recorded at 298 K on a Bruker ESP 300 spectrometer in order to observe the oxidation state of molybdenum in the MoMCM-41 samples. DPPH ($g = 2.0036$) was used as a standard for calculating the g value.

Infrared (IR) spectra were recorded using a MIDAC 101025 FTIR spectrometer in the range 4000–400 cm^{-1} using KBr powder containing ca. 1 wt% of samples.

Diffuse reflectance spectra (UV/vis DRS) were recorded from 240 to 500 nm wavelength on a Shimadzu UV-2401PC spectrophotometer. Samples were pressed 1.5–2 mm thick on a DRS cell and analyzed using $BaSO_4$ and pure silica MCM-41 as a reference.

2.3. Catalytic experiments

The synthesized MoMCM-41 catalysts were tested to check their activity in the oxidation of propylene by using a quartz tube as a fixed-bed flow reactor. Samples of 400 mg were put into the quartz tube (diameter of 16 mm and height of 200 mm) equipped with a sintered quartz disk and then pretreated to 673 K under nitrogen flow at atmospheric pressure for 1 h. The reaction was carried out at 673 K and at atmospheric pressure. The reaction products were analyzed by on-line gas chromatography (CHROMPACK CP9001) on a Carboxen 20M packed column of 1/8 inch diameter and 7.5 ft length with TCD and a Poraplot Q capillary column of 25 m with FID.

3. Results and discussion

3.1. Characterization

Figure 1 shows XRD patterns of calcined MoMCM-41 catalysts with different Si/Mo ratios. The tool spacings are shown in table 1. It can be noted that purely siliceous

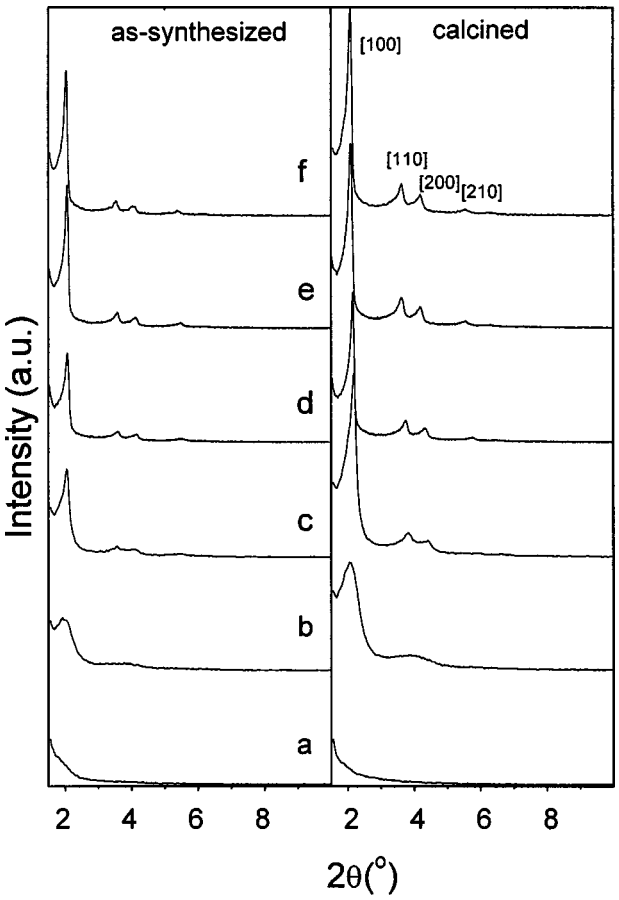

Figure 1. X-ray diffraction patterns of various MoMCM-41 catalysts: (a) MoM1(1), (b) MoM1(3), (c) MoM1(10), (d) MoM1(20), (e) MoM1(50) and (f) MCM-41.

Table 1
Comparison of samples with different Si/Mo ratios.

Sample	Si/Mo (gel mixture)	Si/Mo[a] (product)	d_{100} (nm) calcined	Structure
MCM-41	∞	∞	4.34	Hexagonal
MoM1(50)	50	66	4.29	Hexagonal
MoM1(20)	20	32	4.26	Hexagonal
MoM1(10)	10	17	4.06	Hexagonal
MoM1(3)	3	86	(4.28)	Not defined[b]
MoM1(1)	1	49	no	Amorphous

[a] By AA.
[b] We suggest that it may be a disordered structure.

MCM-41 exhibits the typical hexagonal lattice corresponding to that reported by Beck [2]. It shows four low-angle peaks in the region $2\theta = 1.5$–10, corresponding to the (100), (110), (200) and (210) reflections. It is important to mention that depending on the synthesis conditions, type of silicon and molybdenum sources the position of the main peak may vary significantly. With the decrease of Si/Mo ratio or the increase in molybdenum content of the samples, the spacing of the (100) peak decreases from 4.34 nm of purely siliceous MCM-41 to 4.06 nm of MoMCM-41 with Si/Mo ratio of 17. The observed decrease in interplanar spacing might be explained by the decrease in wall

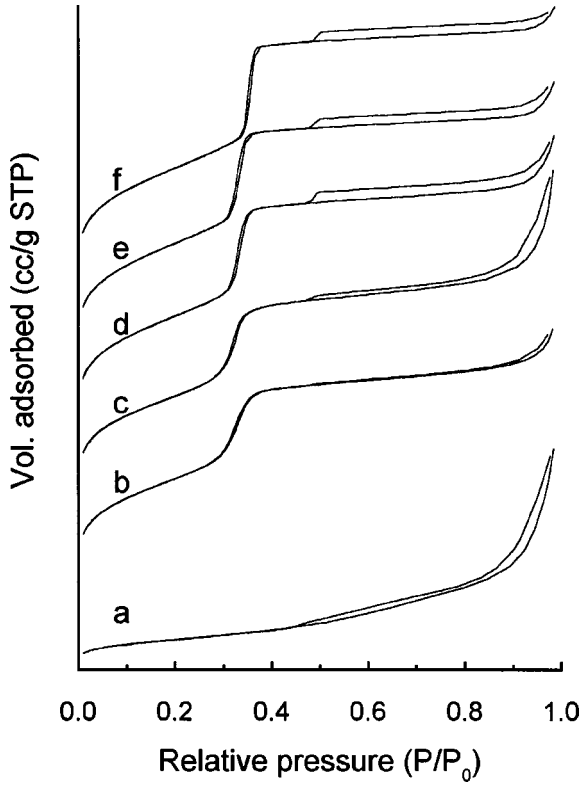

Figure 2. N_2 adsorption–desorption isotherms of various MoMCM-41 catalysts: (a) MoM1(1), (b) MoM1(3), (c) MoM1(10), (d) MoM1(20), (e) MoM1(50) and (f) MCM-41.

thickness of MoMCM-41 catalysts (see table 1) and/or on the basis of replacement of longer Si–O bonds (1.60 Å) by shorter Mo–O bonds in the MCM-41 structure. However, we did not observe any significant changes in wall thickness ($t = a - d_p$, $a = 2/\sqrt{3}\,d_{100}$). The wall thickness was almost 2.1 nm for the synthesized hexagonal structure in this study. On the other hand, with the increase in molybdenum content of the catalysts the (100) diffraction peak becomes broader and less intense. It is suggested that the change of the T–O–T bond angle due to molybdenum incorporation into the framework structure of MCM-41 result in a distortion of the long-range ordering of the hexagonal mesoporous structure and the disappearance of the (110) and (200) diffractions. This distortion was very significant when the Si/Mo ratio of the starting mixture was below 10. We suggested that the maximum content of molybdenum that could be incorporated into the MCM-41 material without destruction of the mesopore structure be about 10 wt%. At higher content the hexagonal structure was not formed and in case of a very high content of molybdenum (Si/Mo = 1, initial) an amorphous structure was formed.

Figure 2 shows the N_2 adsorption–desorption isotherms of the samples. In accordance with those of MCM-41 materials, all samples except MoM1(1) exhibit a well-expressed hysteresis loop of type IV [31]. However, as the initial Si/Mo ratio of synthesis decreases the hysteresis for mesopore was broad, and finally it disappeared. When the initial

Table 2
Nitrogen physisorption data of MoM1 samples.

Sample	Surface area ($m^2\,g^{-1}$)		Pore volume ($cm^3\,g^{-1}$)		Pore diameter[a] (Å)
	BET[b]	Mesopore[c]	Total[d]	Mesopore[c]	
MCM-41	1002	940	0.952	0.803	28.5
MoM1(50)	992	925	0.940	0.776	28.6
MoM1(20)	945	874	0.910	0.725	27.9
MoM1(10)	840	733	0.903	0.657	26.0
MoM1(3)	782	686	0.752	0.534	25.7
MoM1(1)	197	–	0.615	–	–

[a] The pore diameter showing maximum dV/dD in BJH desorption pore distribution.
[b] BET area was calculated by the BET equation for N_2 adsorption isotherms in the range of $P/P_0 = 0.05$–0.2.
[c] The mesopore area and volume with pore diameter below 4.0 nm were calculated by t-plots [32].
[d] Total pore volume measured at $P/P_0 = 0.99$.

content of molybdenum was high, the mesopore structure was not formed. Therefore, the MoM1(1) sample revealed typical amorphous silica. The pore size distribution by the BJH method [30] also showed the same result. As the initial Si/Mo ratio of synthesis decreases the quantity of mesopores decreased. In the case of MoM1(1), no mesopores appeared. These results were in accord with the XRD results.

Table 2 shows pore structural data of the MoMCM-41 catalysts, which were obtained by nitrogen physisorption. We note that the specific surface area and pore volume in the mesopores decrease with the increase of the molybdenum content. The decrease in the mesopore surface area and volume can be explained by the destruction of the pore structure of MoMCM-41 catalysts and/or by the increase of pore wall thickness. However, the increase of pore wall thickness was not observed. The percentage of mesopore surface area in total surface area decreases with the decrease of Si/Mo ratio of initial composition, suggesting that the size of mesopores for the sample with low molybdenum content is more uniform than that for the sample with high molybdenum content. From these results, we can conclude that adding molybdenum in the synthesis system will result in scattering of the mesopore distribution. With the increase of the molybdenum content the effect of the scattering becomes more apparent resulting in poorly hexagonal crystalline materials, which is in agreement with the results of XRD. Large pores may be formed between crystallites and contribute more pore volume than pore surface area.

Figure 3 shows the ESR spectra of MoMCM-41. These spectra also indicate the incorporation of molybdenum into the MCM-41 framework. In the spectrum of MoMCM-41 measured at RT, a signal appears at $g = 2.1$ which is assigned to Mo^{5+}. The hexavalent molybdenum species is not paramagnetic and gives no ESR signal. Both pentavalent and tetravalent molybdenum species are paramagnetic, but the ESR signal due to Mo^{4+} is likely to be very broad and not detectable at room temperature, while the resonance absorption due to Mo^{5+}, in a suitable environment, is readily observable even at room temperature. It is suggested

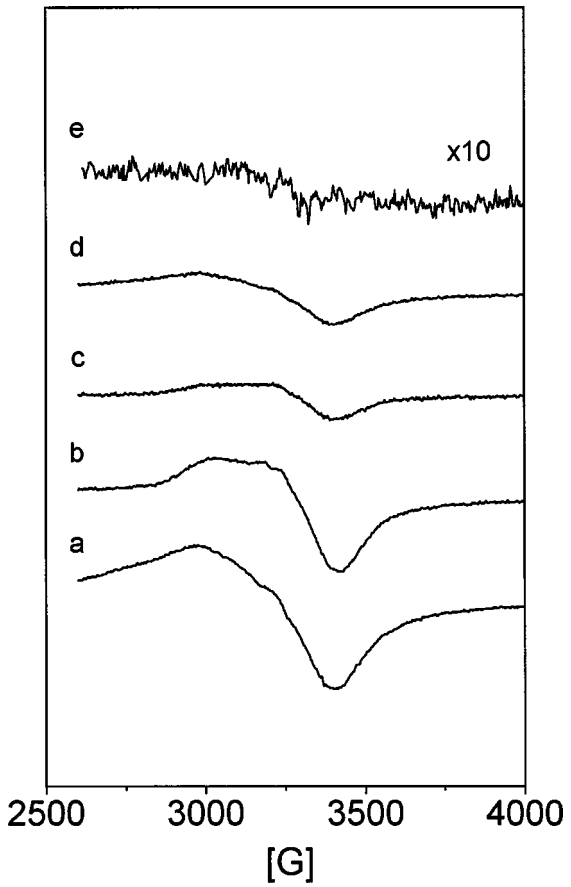

Figure 3. ESR spectra of calcined MoMCM-41 catalysts: (a) MoM1(10), (b) MoM1(20), (c) MoM1(50), (d) MoM1(3) and (e) MoM1(1).

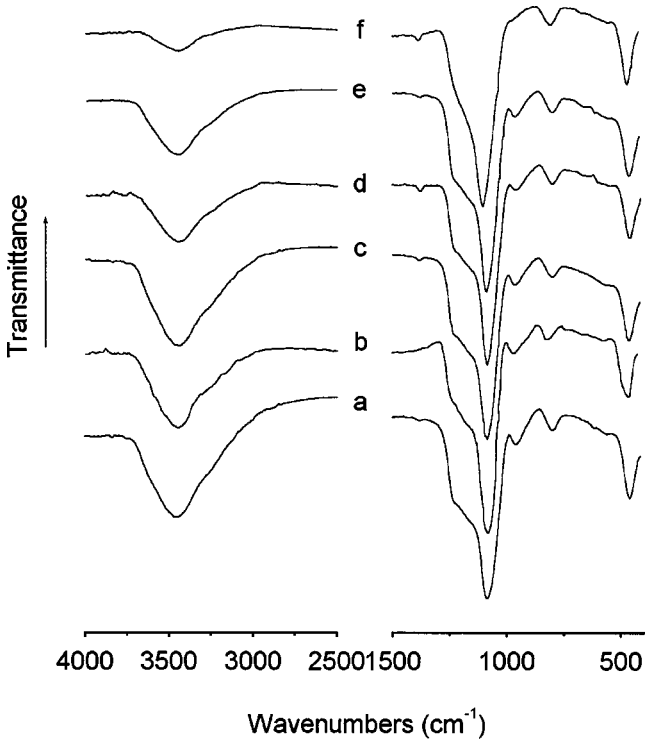

Figure 4. FTIR spectra of calcined MoMCM-41 catalysts: (a) MCM-41, (b) MoM1(10), (c) MoM1(20), (d) MoM1(50), (e) MoM1(3) and (f) MoM1(1).

that the pentavalent state of molybdenum may appear by the Mo–O–Si bond when the molybdenum is incorporated in the MCM-41 structure. Therefore, an ESR signal is observed at a g value of ca. 2.07, which is due to Mo^{5+} in an environment of axial symmetry. In figure 3, we could observe signal peaks of all samples except the MoM1(1) catalyst. As mentioned above, the MoM1(1) catalyst has scarcely any Mo–O–Si bond. In addition, we thought that the MoM1(1) catalyst had MoO_3 crystallites and we could confirm these by FT-IR and UV/vis DRS. However, in XRD analysis of the MoM1(1) catalyst we could not observe any peak of MoO_3 in the range above 10° because of the detection limit of XRD [26]. The signal intensities in the spectra for samples in this figure are depicted based upon the atomic concentration of molybdenum and can directly be used for comparing the concentrations of the paramagnetic species. The intensities of the Mo^{5+} ESR signal for the MoMCM-41 catalysts increase with molybdenum loading.

The IR spectra of MoMCM-41 samples are given in figure 4. The spectra closely resemble that of siliceous MCM-41; the asymmetric and symmetric stretching vibration bands of framework Si–O–Si bonds appear at 1086 and 804 cm^{-1}. For V-containing MCM-41, the band associated with the asymmetric stretching frequency of framework Si–O–Si bonds shifts to a lower frequency region according to the incorporation of vanadium into the MCM-41 framework [33]. However in this study, it was not observed that the band of framework Si–O–Si bonds shifts according to the incorporation of molybdenum into the MCM-41. The interpretation of the band around 960 cm^{-1} has been a matter of debate. This band has been assigned to a stretching vibration mode of a [SiO_4] unit bonded to a titanium ion in titanosilicate or to a vanadium ion in vanadosilicate molecular sieves [33], later to a stretching vibration of Mo=O [34–36]. Recently, it has been suggested that this band is not associated with a metal–oxygen band but can be assigned to Si–O–H stretching at defect sites [37,38]. For pure silicate materials this band has been assigned to the Si–O stretching vibrations of $Si–O^-R^+$ groups, as $R^+ = H^+$ in the calcined pure silicate materials [39]. Therefore, it is thought to be possible that these criteria can be used to ascertain the incorporation of the metal into the structure. In this study, the band at around 960 cm^{-1} is clearly visible in all spectra, except for the MoM1(1) catalyst. The band of Si–O–H stretching at defect sites appeared at 963 cm^{-1} on MCM-41, and at 961–965 cm^{-1} on MoMCM-41 catalysts, except for MoM1(1). However, the shift of a band position indicating the weakening of the Si–O bond by the electropositive Mo ions due to the increasing of defect sites by the molybdenum incorporation was not observed. Even if molybdenum were incorporated into the MCM-41 framework, –OH remained on MoMCM-41 (at 3440 cm^{-1}), then the band shift may almost not be appeared. Otherwise, the band at around 963 cm^{-1} that could be assigned to Si–O–H stretching at defect sites was not observed on the MoM1(1) catalyst. It can be remarked

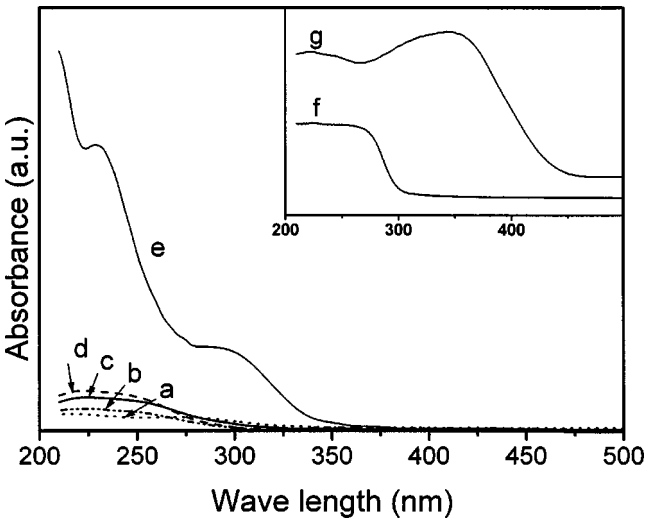

Figure 5. UV-vis diffuse reflectance spectra of calcined MoMCM-41 catalysts: (a) MoM1(3), (b) MoM1(50), (c) MoM1(20), (d) MoM1(10) and (e) MoM1(1). Insert spectra: (f) solid Na_2MoO_4 and (g) solid MoO_3.

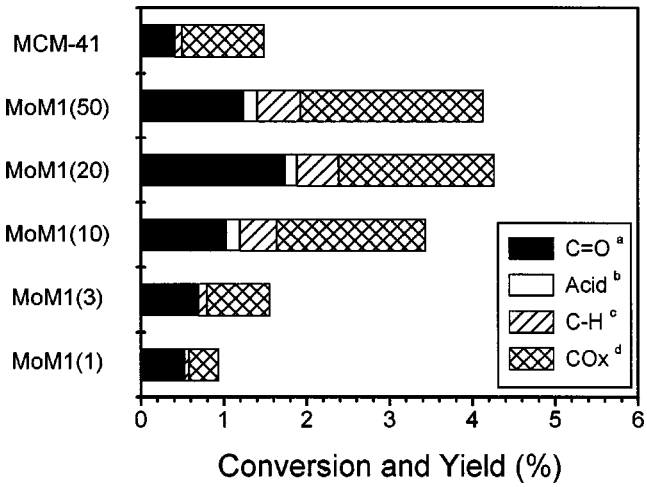

Figure 6. Propylene conversion and product distribution in the oxidation of propylene over MoMCM-41 catalysts at 673 K, $C_3H_6/O_2/N_2 = 6/13/81$ and WHSV $= 2000\ \mathrm{ml\,g^{-1}\,h^{-1}}$: (a) acetaldehyde and acrolein; (b) acetic acid and acrylic acid; (c) CH_4, C_2H_4, C_2H_6 and (d) CO and CO_2.

that the MoM1(1) catalyst, unlike the other catalysts, having no peak around 963 cm^{-1}, has almost no Si–O–H stretching at defect sites. The absence of the Si–OH bond is related to a small peak around 3440 cm^{-1}, a stretching vibration of O–H. Therefore, it is suggested that the MoM1(1) catalyst is amorphous silica that has no defect sites. In the MoM1(1) catalyst, we consider that the molybdenum was almost not incorporated into the MCM-41 framework and only a small amount of molybdenum loaded on MCM-41 may be existent as MoO_3. It should be pointed out that MoO_3 gives two strong bands at 865 and 990 cm^{-1} [40], but no band related to MoO_3 was detected in this IR study in the MoM1(1) catalyst because of low Mo contents [41].

Figure 5 shows the ultraviolet diffuse reflectance spectra between 200 and 500 nm for the MoM1 samples. Since the Mo^{6+} ion has a d^0 electronic configuraton, the absorption band that can occur in the UV-visible range of the electronic spectra is due to the ligand–metal charge transfer. This type of band is usually observed between 200 and 400 nm [42]. All the MoMCM-41 catalysts, except the MoM1(1), exhibited bands at 230–270 nm and the MoM1(1) catalyst exhibited bands at 230 and 300 nm. In addition, MoMCM-41catalysts except the MoM1(1), despite of their Mo concentration being larger than the Mo concentration of the MoM1(1), exhibited clearly smaller peak intensities than the MoM1(1) catalyst due to the small amount of Mo^{6+}. It can be deduced that in the MoM1(1) catalyst all Mo species existed as a form of Mo^{6+}, otherwise in MoMCM-41 catalysts, except the MoM1(1), almost all of the Mo existed as a form of Mo^{5+}. These results are in good agreement with the ESR results.

Even if the absorption peak was very small, the samples, except the MoM1(1), had the bands at 230–270 nm which increase in intensity with increasing molybdenum loading. These bands correspond to Mo^{6+} ions surrounded by oxygen anions in tetrahedral symmetry [43]. In the sample MoM1(1) an absorption band was observed at around 300 nm assigned for octahedral coordination of Mo^{6+} such as polymolybdena clusters of MoO_3 crystallites, but no diffraction peak of MoO_3 was found in XRD patterns [40,44–47]. Another prominent absorption band at around 230 nm in the sample MoM1(1) may be assigned to the octahedral Mo^{6+}. Because there was almost no band at 250–280 nm indicating the tetrahedral Mo^{6+} the band at around 230 nm seemed not to indicate the tetrahedral Mo^{6+} but to indicate the octahedral Mo^{6+}.

3.2. Catalytic activity

We have investigated the catalytic performances of MoMCM-41 catalysts for producing acrolein at conversions of propylene (0.9–4.2%). Figure 6 shows the conversion of propylene and the yields of products in the propylene oxidation over MoMCM-41 catalysts. Under this reaction condition, non-catalytic auto-oxidation of propylene in the empty reactor could be ignored. We can observe the effect of the incorporation amount of molybdenum into MCM-41 on the propylene oxidation. When molybdenum is incorporated into the MCM-41 the activity is increased. Among the catalysts tested, the highest selectivity to oxygenates was obtained over the MoM1(20) catalyst with a relatively high oxygenate yield. In case of the MoM1(1) catalyst, nevertheless it has 3.1 wt% molybdenum the activity is very low. This may be due to the structure like low surface area, as shown in tables 1 and 2, or due to whether a framework Mo was formed or not. Since the activity is observed at low value on MoM1(1) which has a very high intensity for Mo^{6+} as a result of UV/vis analysis, the octahedral site of Mo^{6+} seemed not to have an important role on propylene oxidation in these MoMCM-41 catalysts. In addition, the activity seemed not to depend on the structure because the catalyst having high crystallinity and high surface area did not show high activity. The catalysts that according to the ESR spectra had Mo^{5+} species that can be considered as

framework Mo (all catalysts except the MoM1(1)) show relatively high catalytic activies. Then, it is supposed that Mo^{5+}species in these MoMCM-41 catalysts has a possibility to act as an active site.

4. Conclusions

MoMCM-41 catalysts having well-developed hexagonal structure were synthesized. It was invested that the maximum content of molybdenum that could be synthesized without destruction of the mesopores by direct synthesis method was about 10 wt%. At the above Si/Mo = 10 (initial) the hexagonal structure was not formed and in case of a relatively high content of molybdenum (Si/Mo = 1, initial) an amorphous structure was formed. The molybdenum species at MoMCM-41 having hexagonal structure was in existence by Mo^{5+}. The molybdenum thought to be incorporated into a framework of MCM-41. It is worth pointing out that, the catalytic activity for propylene oxidation on the MoMCM-41 catalysts including Mo^{5+} was higher than that not including Mo^{5+} and was obtained at the highest value on the catalyst having about 3 wt% molybdenum.

Acknowledgement

This research was supported by KRICT program (kk 9905-02).

References

[1] C.T. Kresge, M.E. Leonowicz, W.J. Roth and J.C. Vartuli, US Patent No. 5,098,689 (1992).
[2] J.S. Beck, US Patent No. 5,057,296 (1991).
[3] J.S. Beck, J.C. Vartuli, W.J. Roth, M.E. Leonowicz, C.T. Kresge, K.D. Schmitt, C.T.-W. Chu, D.H. Oslon, E.W. Sheppard, S.B. McCullen, J.B. Higgins and J.L. Schlenker, J. Am. Chem. Soc. 114 (1992) 10834.
[4] C.Y. Chen, H.X. Li and M.E. Davis, Micropor. Mater. 2 (1993) 17.
[5] R.B. Borade and A. Clearfield, Catal. Lett. 31 (1995) 267.
[6] Z. Luan, C.-F. Cheng, W. Zhou and J. Klinowski, J. Phys. Chem. 99 (1995) 1018.
[7] A. Corma, M.T. Navarro and J. Perez Pariente, J. Chem. Soc. Chem. Commun. (1994) 147.
[8] K.M. Reddy, I. Moudrakovski and A. Sayari, J. Chem. Soc. Chem. Commun. (1994) 1059.
[9] Z. Luan, J. Xu, H.Y. He, J. Klinowski and L. Kevan, J. Phys. Chem. 100 (1996) 19995.
[10] D. Trong On, P.N. Joshi and S. Kaliaguine, J. Phys. Chem. 100 (1996) 6743.
[11] A. Sayari, I. Moudrakovski, C. Danumah, C.I. Ratclitte, J.A. Ripmeester and K.F. Preston, J. Phys. Chem. 99 (1995) 16373.
[12] D.Y. Zhao and D. Goldfarb, J. Chem. Soc. Chem. Commun. (1995) 875.
[13] D.Y. Zhao and D. Goldfarb, in: *Zeolites: A Refined Tool for Designing Catalytic Sites*, eds. L. Bonneviot and S. Kaliaguine (Elsevier, Amsterdam, 1995) p. 181.
[14] D.M. Antonelli and J.Y. Ying, Chem. Mater. 8 (1996) 874.
[15] A. Poppl, M. Newhouse and L. Kevan, J. Phys. Chem. 99 (1995) 10019.
[16] Z.Y. Yuan, S.Q. Liu, T.H. Chen, J.Z. Wang and H.X. Li, J. Chem. Soc. Chem. Commun. (1995) 973.
[17] N. Ulagappan and C.N.R. Rao, J. Chem. Soc. Chem. Commun. (1996) 1047
[18] C.-F. Cheng, H. He, W. Zhou and J. Klinowski, J. Phys. Chem. 100 (1996) 390.
[19] A. Poppl, P. Baglioni and L. Kevan, J. Phys. Chem. 99 (1995) 14156.
[20] A. Poppl and L. Kevan, Langmuir 11 (1995) 4486.
[21] A. Poppl, M. Hartmann and L. Kevan, J. Phys. Chem. 99 (1995) 17251.
[22] V. Luca, D.J. MacLachlan, R. Bramley and K. Morgen, J. Phys. Chem. 100 (1996) 1793.
[23] M. Hartman, A. Poppl and L. Kevan, J. Phys. Chem. 99 (1995) 17494.
[24] W. Zhang, J. Wang, P.T. Tanev and T.J. Pinnavaia, J. Chem. Soc. Chem. Commun. (1996) 979.
[25] S. Ayyappan and N. Ulagappan, Proc. Indian Acad. Sci. (Chem. Sci.) 108 (1996) 505.
[26] M. Cheng, F. Kumata, T. Saito, T. Komatsu and T. Yashima, in: *Mesoporous Moleclar Sieves 1998*, eds. L. Bonneviot, F. Beland, C. Danumah, S. Giasson and S. Kaliaguine (Elsevier, Amsterdam, 1998) p. 485.
[27] A. Corma, A. Martinez, V. Martinez-Soria and J.B. Monton, J. Catal. 153 (1995) 25.
[28] T. Klimova, J. Ramirez, M. Calderon and J.M. Dominguez, in: *Mesoporous Moleclar Sieves 1998*, eds. L. Bonneviot, F. Beland, C. Danumah, S. Giasson and S. Kaliaguine (Elsevier, Amsterdam, 1998) p. 493.
[29] R. Ryoo and S. Jun, J. Phys. Chem. B 101 (1997) 317.
[30] E.P. Barret, L.G. Joyner and P.P. Halenda, J. Am. Chem. Soc. 73 (1951) 373.
[31] S. Brunauer, L.S. Deming, W.S. Deming and E. Teller, J. Am. Chem. Soc. 62 (1940) 1723.
[32] W.D. Harkins and G. Jura, J. Am. Chem. Soc. 66 (1944) 1362.
[33] Z. Luan, J. Xu, H. He, J. Klinowski and L. Kevan, J. Phys. Chem. 100 (1996) 19595.
[34] M. Akimoto and E. Echigoya, Chem. Lett. (1981) 1759.
[35] K. Eguchi, Y. Toyozawa, N. Yamazoe and T. Seiyama, J. Catal. 83 (1983) 32.
[36] N. Mizuno, K. Katamura, Y. Yoneda and M. Misono, J. Catal. 83 (1983) 384.
[37] M.A. Camblor, A. Corma and J. Perez Pariente, J. Chem. Soc. Chem. Commun. (1993) 557.
[38] P.S. Raghavan and M.P. Vinod, J. Mol. Catal. A 135 (1998) 47.
[39] T. Blasco, A. Corma, M.T. Navarro and J. Perez Pariente, J. Catal. 156 (1995) 65.
[40] N. Giordano, J.C.J. Bart, A. Vaghi, A. Castellan and G. Martinotti, J. Catal. 36 (1975) 81.
[41] C. Rocchiccioli-Deltcheff, M. Amirouche, M. Che, J.-M. Tatibouet and M. Fournier, J. Catal. 125 (1990) 292.
[42] M. Fournier, C. Louis, M. Che, P. Chaquin and D. Masure, J. Catal. 119 (1989) 400.
[43] M.A. Banares and J.L.G. Fierro, Catal. Lett. 17 (1993) 205.
[44] J.H. Ashley and P.C.H. Mitchell, J. Chem. Soc. A (1969) 2730.
[45] M. Che, F. Figueras, M. Forissier, J.C. McAteer, M. Perrin, J.L. Portefaix and H. Praliaud, in: *Proc. 6th Int. Congr. Catal.*, London, 1976, Vol. 1, eds. G.C. Bond, P.B. Wells and F.C. Tompkins (The Chemical Society, London, 1977) p. 261.
[46] P. Gajardo, D. Pirotte, P. Grange and B. Delmon, J. Phys. Chem. 83 (1979) 1780.
[47] L. Wang and W.K. Hall, J. Catal. 77 (1982) 232.